Constructing Hopf bifurcation lines for the stability of nonlinear systems with two time delays

Romain Modeste Nguimdo
Optique Nonlinéaire Théorique, Université Libre de Bruxelles, Campus Plaine, CP 231, 1050 Bruxelles, Belgium

(Received 30 October 2017; published 21 March 2018)

Although the plethora real-life systems modeled by nonlinear systems with two independent time delays, the algebraic expressions for determining the stability of their fixed points remain the Achilles' heel. Typically, the approach for studying the stability of delay systems consists in finding the bifurcation lines separating the stable and unstable parameter regions. This work deals with the parametric construction of algebraic expressions and their use for the determination of the stability boundaries of fixed points in nonlinear systems with two independent time delays. In particular, we concentrate on the cases for which the stability of the fixed points can be ascertained from a characteristic equation corresponding to that of scalar two-delay differential equations, one-component dual-delay feedback, or nonscalar differential equations with two delays for which the characteristic equation for the stability analysis can be reduced to that of a scalar case. Then, we apply our obtained algebraic expressions to identify either the parameter regions of stable microwaves generated by dual-delay optoelectronic oscillators or the regions of amplitude death in identical coupled oscillators.

DOI: 10.1103/PhysRevE.97.032211

I. INTRODUCTION

Systems with two independent delays are ubiquitous in many areas of science and engineering, including electronics [1], photonics (e.g., optoelectronic oscillators (OEOs) [2,3]), collective behaviors [4], and many others [5–13]. In network of coupled oscillators, for example, two independent delays arise due to both the communication delay between the individual elements [14–17] and processing delay required for handling input information or to respond to sudden changes of parameters [4]. Dual-delay feedback loops also can be implemented deliberately in dynamical systems for stabilizing unstable periodic orbits or unstable fixed points [18]. In communication systems, radars, sensors, metrology, and OEOs with two time-delay feedback loops are excellent sources for generating ultrapure microwaves. In all cases, however, the construction of analytical solutions to analyze their stability is very challenging although characteristic equations can be easily formulated. This difficulty is due to the fact that the presence of delay even in the simplest mathematical model brings the system to an infinite dimension although only a finite number of dynamical variables is involved. Even for the stability of basic solutions such as the origin or nontrivial steady state solutions, it is extremely difficult to derive general algebraic expressions for their stability.

Alternatively, the determination of Hopf bifurcation lines of the steady state solutions is sufficient to draw the boundaries separating the stable regions from the unstable ones. For systems with single time delay, the stability condition for defining the primary Hopf bifurcation lines can be found [1,19,20]. For example, the stability analysis of pure microwaves generated by single delay OEOs has been analytically derived either under some assumptions [21] or in a parametric form [22,23]. Also, for nonlinear coupled oscillators with single delay, there are analytical expressions which can be efficiently used to identify the parameter regions for some interesting dynamical regimes such as amplitude death (AD) [24–27].

For systems with two independent delays, however, most of comprehensive bifurcation analyses for determining the stability of the steady states have been studied numerically rather than purely algebraic [1,4,9,10,18,28]. A geometric approach also has been proposed [29]. A few attempts for algebraic expressions to determine eigenvalues in such cases have consisted in expanding eigenvalue in orders of the inverse of the time delay [30]. But, the latter approach cannot be applied to the dual feedback cases for which the order of magnitude of the second time delay can vary in comparison to the first.

The present work is devoted to further investigations on the algebraic generic expressions for identifying the boundaries between stable and unstable parameter regions of a given fixed point of nonlinear systems with two independent time delays. A parametric approach is used to construct the time-delay expressions from which such boundaries can be drawn. This parametric approach has been applied to several one-delay systems [22,23]. Here, we extend this method to the case of nonlinear systems with two time delays. A special attention is paid to the application of the obtained results to real-world systems. In particular, we consider several diffusively coupled oscillators with two time delays and dual-delay loop OEOs, and use the constructed expressions to identify the parameter regions in which either stable microwaves or amplitude death can be found.

II. ALGEBRAIC FORMULAS FOR IDENTIFYING BIFURCATION LINES

In most of the nonlinear systems with two time delays, the characteristic equation to ascertain the stability of their fixed points has the form [1–6,8–10]

$$\mathcal{R}_1(\lambda)e^{-\lambda T_1} + \mathcal{R}_2(\lambda)e^{-\lambda T_2} = Q(\lambda), \quad (1)$$

where $\lambda \in \mathbb{C}$ denotes the zeros of Eq. (1), T_1 and T_2 are independent time delays; $\mathcal{R}_1(\lambda), \mathcal{R}_2(\lambda) \in \mathbb{C}$ and $Q(\lambda)$ are complex functions independent of time delay. The explicit expressions of these complex functions depend on the physical system under study. They can be polynomials in λ or any arbitrary complex function of λ independent of time delays. The considered characteristic equation corresponds either to the case of scalar delay differential equations, one-component delay feedback, or to delay differential equations that can be reduced to a scalar case. Because of the exponential terms, it is extremely difficult to find all the roots of Eq. (1). Despite this fact, the potential values at which the stability of the fixed point may change are obtained when λ crosses the imaginary axis. Hence, to find the bifurcation points at which the change in the stability occurs, we insert $\lambda = i\omega$ into Eq. (1). Considering $\mathcal{R}_1(i\omega) = R_1(\omega)e^{i\theta_1(\omega)}$, $\mathcal{R}_2(i\omega) = R_2(\omega)e^{i\theta_2(\omega)}$, and $Q(i\omega) = Q_1(\omega) + iQ_2(\omega)$, and by separating the real and imaginary parts, we obtain

$$\begin{aligned} R_1 \cos\left(\omega T_1^{\text{cr}} - \phi_1\right) &= Q_1 - R_2 \cos\left(\omega T_2^{\text{cr}} - \phi_2\right), \\ R_1 \sin\left(\omega T_1^{\text{cr}} - \phi_1\right) &= -Q_2 - R_2 \sin\left(\omega T_2^{\text{cr}} - \phi_2\right), \end{aligned} \tag{2}$$

where T_1^{cr} and T_2^{cr} are the critical time delays for which the system loses its stability or instability. Equation (2) can be parametrically solved with respect to the parameter ω to determine the expression of ωT_2^{cr}:

$$\begin{aligned} \omega T_2^{\text{cr}} = &\pm \arccos\left(\frac{Q_1^2 + Q_2^2 - R_1^2 + R_2^2}{2R_2\sqrt{Q_1^2 + Q_2^2}}\right) \\ &- \arctan\left(\frac{Q_2}{Q_1}\right) + \phi_2 + 2k\pi, \end{aligned} \tag{3}$$

where k is integer. The sign $(\pm)$ in Eq. (3) indicates that two possible expressions of ωT_2^{cr} can be obtained. While any value of k can be used, we are only interested in the smallest possible value of k for which ωT_2^{cr} is a nonnegative value. However, it should be noted that there is no value of ωT_2^{cr} when the following inequality is not satisfied:

$$\left|\frac{Q_1^2 + Q_2^2 - R_1^2 + R_2^2}{2R_2\sqrt{Q_1^2 + Q_2^2}} \equiv \mathcal{U}\right| \leqslant 1. \tag{4}$$

This means that the values of ω to be considered are those for which the condition given in Eq. (4) is satisfied. Since the sum $Q_1^2 + Q_2^2$ is a positive quantity, condition (4) can be rewritten as

$$(R_1 - R_2)^2 \leqslant Q_1^2 + Q_2^2 \leqslant (R_1 + R_2)^2. \tag{5}$$

Several scenarios are possible depending on R_1 and R_2. If R_1 and R_2 are such that there is no value of ω verifying the inequality given in Eq. (5), the concerned steady state is always stable or unstable. Condition (5) is important as it allows one to identify the value range in which ω should be scanned to find the appropriate values of T_2^{cr}. This simplifies the scan as compared to the case for which the critical time delays are found numerically from the characteristic equation.

Similarly, ωT_1^{cr} also can be determined from Eq. (2). One obtains

$$\begin{aligned} \omega T_1^{\text{cr}} = &\pm \arccos\left(\frac{Q_1^2 + Q_2^2 + R_1^2 - R_2^2}{2R_1\sqrt{Q_1^2 + Q_2^2}}\right) \\ &- \arctan\left(\frac{Q_2}{Q_1}\right) + \phi_1 + 2p\pi, \end{aligned} \tag{6}$$

where p is integer. It must be emphasized that Eq. (6) should satisfy the same existence condition (5). Under the condition that both Eqs (3) and (6) satisfy condition (5), Eqs. (3) and (6) yield

$$\begin{aligned} T_1^{\text{cr}}(\omega) = &\frac{\phi_1}{\omega} \pm \frac{1}{\omega} \arccos\left(\frac{Q_1^2 + Q_2^2 + R_1^2 - R_2^2}{2R_1\sqrt{Q_1^2 + Q_2^2}}\right) \\ &- \frac{1}{\omega} \arctan\left(\frac{Q_2}{Q_1}\right) + \frac{2p\pi}{\omega}, \end{aligned} \tag{7}$$

$$\begin{aligned} T_2^{\text{cr}}(\omega) = &\frac{\phi_2}{\omega} \pm \frac{1}{\omega} \arccos\left(\frac{Q_1^2 + Q_2^2 - R_1^2 + R_2^2}{2R_2\sqrt{Q_1^2 + Q_2^2}}\right) \\ &- \frac{1}{\omega} \arctan\left(\frac{Q_2}{Q_1}\right) + \frac{2k\pi}{\omega}. \end{aligned} \tag{8}$$

The pair of expressions (7) and (8) are the key formulas for determining the bifurcation lines delimiting the stable and unstable regions for any fixed point whose stability can be ascertained from Eq. (1). However, it should be noted that, among the values of T_1^{cr} and T_2^{cr} obtained from Eqs. (7) and (8), only those satisfying the relations in Eq. (2) are of interest since expressions (7) and (8) have been obtained by squaring the terms in Eq. (2). It also should be noted that because of the sign $(\pm)$ in Eqs. (7) and (8), stable and unstable regions can be bounded by up to four curves for some systems. One important result of this paper is that the critical values of T_1^{cr} and T_2^{cr} are algebraically determined simultaneously. In addition, expressions (7) and (8) are valid even when the coefficients of the transcendental terms (i.e., $\mathcal{R}_1$ and $\mathcal{R}_2$) are complex nonpolynomial functions in ω. Next, we consider various wide studied physical systems and apply the formulas (7) and (8) to ascertain the stability of their fixed points.

III. STABILITY ANALYSIS OF NONLINEAR SYSTEMS WITH TWO TIME DELAYS

A. Stability of dual-delay loop optoelectronic oscillators

In usual delay OEOs, a laser beam with constant power is used to seed an electro-optic modulator [typically a Mach-Zehnder modulator (MZM)] that is polarized and modulated in its radio-frequency (rf) electrode by a periodic signal. The output signal of such MZM is subsequently purified traveling through a long optical fiber delay line and/or an optical resonator with a high quality factor. Then, the output of the fiber or resonator is detected using a photodetector and converted back to electrical signal. Finally, the signal at the output of the photodetector is either launched into a rf filter to select the microwave frequency of interest before being applied back to the rf electrode of the MZM or it can be directly applied back to such electrode if the microwave frequency has been selected by the resonator. In the case of dual-loop OEOs, the output of the resonator or fiber is usually split into two parallel optical branches with different delay lengths. Each branch is detected separately and the detected signals are then combined before being applied back to the rf electrode of the MZM. Complicated configurations also have been proposed (e.g., see Ref. [3]). In the modeling of OEOs generating microwaves, the system is assumed weakly nonlinear so that the microwave dynamics described by a dimensionless variable $x(t)$ can be found in the form $x(t) = \frac{1}{2}\mathcal{A}(t)e^{i\Omega_0 t} + \frac{1}{2}\mathcal{A}^*(t)e^{-i\Omega_0 t}$, where $\mathcal{A}(t)$ is the slowly varying complex amplitude ($*$ indicates the complex conjugate) of the microwave while Ω_0 is its frequency. As such, pure microwaves are signals $x(t)$ for which the amplitude $\mathcal{A}$ is a stable fixed point. These fixed points and their stability analysis can be completely investigated from the integrodifferential equations describing the slowly varying complex amplitude $\mathcal{A}(t)$ of the microwave. For ultrapure microwave generation using single or multiple delay OEOs, two types of integrodifferential equations are commonly used for modeling OEOs depending on whether or not a high quality-factor resonator is also inserted in the delay loop.

For dual-loop OEOs without resonator, the two time delays are implemented from two different parallel optical delay paths [3,21]. The microwave frequency is selected using a narrow bandpass rf filter inserted in the electrical branch. Assuming that the slowly varying complex amplitude of the microwaves can be written as $\mathcal{A} = Ae^{i\varphi}$, the dynamics of such a system can be studied by [3]

$$\dot{\mathcal{A}} + \mu\mathcal{A} = \mu\gamma_1 \mathrm{J}_{C1}(2A_{T_1})\mathcal{A}_{T_1} + \mu\gamma_2 \mathrm{J}_{C1}(2A_{T_2})\mathcal{A}_{T_2}, \quad (9)$$

where $F_{T_j} = F(t - T_j)$, γ_j is the effective gain in the delay branch j (with $j = 1,2$), while μ is the half-bandwidth of the narrow-band filter used in the microwave branch. $\mathrm{J}_{c1}(x)$ is the Bessel Cardinal function defined as $\mathrm{J}_{c1}(x) = \mathrm{J}_1(x)/x$, $\mathrm{J}_n(x)$ being the nth-order Bessel functions of the first kind with n as an integer. For $\dot{\mathcal{A}} = 0$, there is a trivial fixed point $A^{\mathrm{st}} = 0$ which exists for every value of the loop gain. Its linear stability can be determined by the following characteristic equation:

$$\lambda + \mu(1 - \gamma_1 e^{-\lambda T_1} - \gamma_2 e^{-\lambda T_2}) = 0. \quad (10)$$

From Eq. (10), one can deduce the parameters in Eqs. (7) and (8) as $\phi_1 = 0$, $\phi_2 = 0$, $R_1 = \gamma_1$, $R_2 = \gamma_2$, $Q_1 = 1$, and $Q_2 = \omega/\mu$. It turns out that the condition in Eq. (4) is fulfilled if and only if

$$(\gamma_1 - \gamma_2)^2 \leqslant 1 + z^2 \leqslant (\gamma_1 + \gamma_2)^2, \quad (11)$$

where $z = \omega/\mu$. From Eq. (11), it is seen that T_1^{cr} and T_2^{cr} do not exist for $(\gamma_1 + \gamma_2) < 1$. This means that there is no value of T_1 and T_2 for which λ crosses the imaginary axis. The fixed point $A^{\mathrm{st}} = 0$ remains stable as it is already the case in the absence of any time delay. For $(\gamma_1 + \gamma_2) \geqslant 1$, we find from formulas (7) and (8) that the fixed point $A^{\mathrm{st}} = 0$ is always unstable.

For $(\gamma_1 + \gamma_2) > 1$, Eq. (9) also has, in addition to the trivial fixed point, a nontrivial steady state solution:

$$A^{\mathrm{st}} = \frac{1}{2}\mathrm{J}_{c1}^{-1}\left[\frac{1}{2(\gamma_1 + \gamma_2)}\right]. \quad (12)$$

The characteristic equation for the growth rate of such fixed point is given by [22]

$$\lambda + \mu(1 - \mathcal{R}_1 e^{-\lambda T_1} - \mathcal{R}_2 e^{-\lambda T_2}) = 0, \quad (13)$$

where $\mathcal{R}_j = \gamma_j[\mathrm{J}_0(2A^{\mathrm{st}}) - \mathrm{J}_2(2A^{\mathrm{st}})]$. It is worth noting that $\mathcal{R}_j$ are real values. The main difference between Eqs (10) and (13) is that the $\mathcal{R}_j$ are positive reals in the former, while they can be positive or negative reals in the latter, depending on the value of A^{st}. From Eq. (13), it turns out that $Q_1 = 1$ and $Q_2 = \omega$, $R_j = \gamma_j|[\mathrm{J}_0(2A^{\mathrm{st}}) - \mathrm{J}_2(2A^{\mathrm{st}})]|$, $\phi_j = 0$ if $\mathcal{R}_j \geqslant 0$; otherwise, $\phi_j = \pi$. Letting $z = \omega/\mu$, Eqs. (7) and (8) degenerate to

$$\mu T_1^{\mathrm{cr}} = \frac{\phi_1}{z} \pm \frac{1}{z}\arccos\left(\frac{1 + z^2 + R_1^2 - R_2^2}{2R_1\sqrt{1+z^2}}\right) - \frac{1}{z}\arctan(z) + \frac{2p\pi}{z},$$
$$\mu T_2^{\mathrm{cr}} = \frac{\phi_2}{z} \pm \frac{1}{z}\arccos\left(\frac{1 + z^2 - R_1^2 + R_2^2}{2R_2\sqrt{1+z^2}}\right) - \frac{1}{z}\arctan(z) + \frac{2k\pi}{z}. \quad (14)$$

Equation (14) gives a family of solutions for different values of z, p, and k. For a system with single time delay (i.e., $\gamma_2 = 0$), the stability analysis has been carried out in Ref. [22]. Our main contribution here is to use Eq. (14) for investigating a potential change in the stability of this fixed point which may be caused by an additional time delay (i.e., T_2). Since Eq. (14) is z dependent, only the minimum values of μT_1^{cr} and μT_2^{cr} are of interest as they give the effective boundary curves separating the stable regions from the unstable ones. These minimum values are found for $\min\{\mu T_1^{\mathrm{cr}}\} \geqslant 0$ and $\min\{\mu T_2^{\mathrm{cr}}\} \geqslant 0$:

$$\mu T_1 < \min\{\mu T_1^{\mathrm{cr}}\},$$
$$\mu T_2 < \min\{\mu T_2^{\mathrm{cr}}\}. \quad (15)$$

Figure 1 depicts the bifurcation lines separating the stable regions from the unstable ones for different values of R_j. No-colored regions correspond to that in which the generated

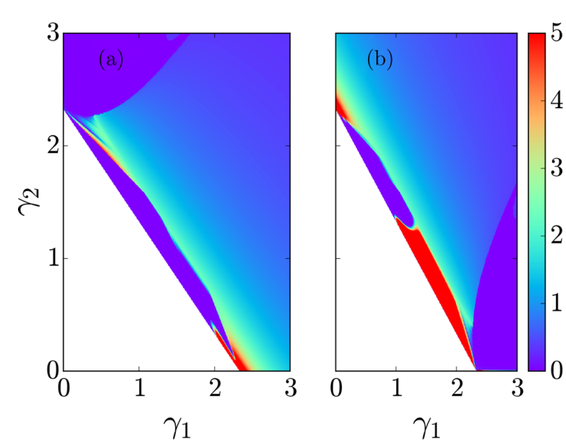

FIG. 1. Necessary and sufficient conditions for asymptotic stability of the nontrivial solution using Eq. (15). The white regions for which $(\gamma_1 + \gamma_2) > 1$ are those in which the microwave amplitudes are asymptotically stable: results for (a) T_1 and (b) T_2. The color scale indicates $\mu T_1 = \min\{\mu T_1^{\mathrm{cr}}\}$ and $\mu T_2 = \min\{\mu T_2^{\mathrm{cr}}\}$.

microwaves are unconditionally stable independent of the time-delay lengths, while the color scale indicates the minimum values of μT_1 and μT_2 above which the time-delay modulated microwaves are generated. Compared to the bifurcation line shown in Ref. [22] for single time delay, our results show that the unconditional stability region does not significantly change although the presence of an additional time delay. The latter can even slightly enlarge it. Through numerical simulations of Eq. (9) (not shown here), we have evidenced a good agreement between analytical and numerical predictions of such stability regions.

For dual-loop OEOs with resonator, an optical resonator with a high quality factor is inserted in the delay loop as well in order to filter out the spurious ring-cavity peaks arising in the radio-frequency spectrum. In such a scheme, the microwave frequency is selected by the resonator instead of the rf filter as in the case of OEOs without resonator. The relevant variables to describe pure microwaves are the slowly varying amplitudes of the complex electric field $\mathcal{G}_n(t)$ attached to different resonator modes and the microwave amplitude $\mathcal{A}(t)$. For resonator-based OEOs with single time-delay loop, the differential equation to describe the dynamics of the slowly varying complex amplitude has been formulated [22,31,32]. In this work, this model is modified such as to account for the second delay loop. One obtains

$$\dot{\mathcal{G}}_n = -(\tau^{-1} + i\sigma)\mathcal{G}_n + \gamma_n(\phi)\mathrm{J}_n(A)e^{in\varphi}, \tag{16}$$

$$\mathcal{A}(t) = 2\sum_{n=-\infty}^{+\infty}\left(\beta_1\mathcal{G}_{n+1,T_1}\mathcal{G}^*_{n,T_1}e^{iv_1} + \beta_2\mathcal{G}_{n+1,T_2}\mathcal{G}^*_{n,T_2}e^{iv_2}\right), \tag{17}$$

with $\mathcal{G}_{n,T} = \mathcal{G}_n(t-T)$. τ is the overall photon lifetime in the resonator; $\sigma = \omega_L - \omega_0$ is the detuning frequency between the laser frequency ω_L and the central frequency of the pumped mode ω_0; β_j ($j = 1,2$) is the optoelectronic gain in the path j when the effect of the resonator is not taken into account; v_j represents the overall microwave round-trip phase shift accumulated in the path j, $\gamma_n(\phi)$ is the effective gain for the mode n, ϕ being the static phase of the nonlinear element used (typically a MZM). To work properly and also to achieve low phase noise performance, the laser frequency ω_L must be tuned and locked to the central frequency ω_0 of the pumped mode of the WGMR [32,33]. Typically, this is turned such that $\sigma \ll \tau^{-1}$. In our previous work on single delay OEO with resonator, we have shown that the stability of the system does not change when $\sigma \ll \tau^{-1}$ [22]. Since this condition should be satisfied even for dual-delay OEOs with resonator, the stability analysis of the fixed points can be ascertained assuming $\sigma \approx 0$. Hence the nontrivial steady state of Eq. (17) is also given by Eq. (12) with $\gamma_j = (4\beta_j\tau^2|\sin(2\phi)|)/(\tau_e\tau_d(1+\sigma^2\tau^2))$, and its linear stability is determined by Eq. (13) with $\mu = \tau^{-1}$, $R_j = \gamma_j[\mathrm{J}_0(2A^{\mathrm{st}}) - \mathrm{J}_2(2A^{\mathrm{st}})]$ [22]. The calculation details for obtaining such characteristic equation are given in the Appendix. It is evident that, despite the different structure of the equations describing the dynamical features of the two subclasses of OEOs, their stability analysis can be studied using the same Eq. (13). Hence the bifurcation lines separating the stable and the unstable regions are also given by Eq. (14) and the results obtained from these formulas are those in Fig. 1.

B. Stability of coupled oscillators with two time delays

In a network of coupled oscillators, several topologies have been proposed. In some of them, the two time delays emerge naturally (i.e., the processing delay δ and the propagation time T) although most of the previous studies only have considered the transmission time T. However, both time delays have been found to play a role for the occurrence of the AD [4]. In other models, the two time delays are implemented deliberately for the control purposes [18]. In these two cases, the boundaries delimiting the AD regions have been found by solving the characteristic equation numerically [4,18]. Here, we illustrate that such numerical results can be analytically obtained from Eqs. (7) and (8). For N-diffusively delay-coupled oscillators having the same natural frequency ω_0, the model is given by [4,24]

$$\dot{Z}_j = (1 + i\omega_0 - |Z_j|^2)Z_j + \frac{K}{d_j}\sum_{s=1}^{N} g_{js}[Z_s(t-\delta-T) - \alpha Z_j(t-\delta)], \tag{18}$$

where Z_j ($j = 1,2,\ldots,N$) is the complex amplitude of the oscillator j; K quantifies the strength of coupling; d_j denotes the degree of oscillator j: $g_{js} = g_{sj} = 1$ (with $s \neq j$) if oscillators j and s are connected and $g_{js} = g_{sj} = 0$ otherwise. α is a factor in the coupling recently introduced in the model for better modeling of the real situations [24]. Performing a standard linear stability analysis of Eq. (18) around the homogeneous steady state (HSS) solution (i.e., $Z_j = 0$) yields the following N characteristic equation:

$$\lambda - i\omega_0 - 1 + \alpha K\, e^{-\lambda\delta} - K\rho_j e^{-\lambda(T+\delta)} = 0, \tag{19}$$

where ρ_j's are eigenvalues of the network matrix $M = (g_{js}/d_j)_{N\times N}$ which are ordered as $\rho_1 = 1$ and $\rho_1 \geqslant \rho_2 \geqslant \cdots \geqslant -1/(N-1) \geqslant \rho_j \geqslant -1$. If all the real parts of the eigenvalues are negative, and the HSS $Z_j = 0$ is linearly stable, then AD occurs. It is known that the boundaries of AD island are defined by only two extreme eigenvalues: $\rho_1 = 1$ and ρ_N. Equation (19) can be matched to Eq. (1) with $Q(\lambda) = 1 - \lambda + i\omega_0$, $\mathcal{R}_1 = \alpha K$, $\mathcal{R}_2 = -K\rho_j$, $T_1 = \delta$, and $T_2 = T + \delta$. This leads to $Q_1 = 1$, $Q_2 = \omega_0 - \omega$, $R_1 = \alpha K$, $\phi_1 = 0$, $R_2 = K|\rho_j|$, and $\phi_2 = \pi$ for $\rho_j > 0$ or $\phi_2 = 0$ for $\rho_j < 0$.

For $T_1 \neq T_2 \neq 0$ (i.e., for $\delta \neq 0$), no theoretical prediction has been previously reported for coupled nonlinear oscillators, even for $N = 2$. Fortunately, our approach allows successful analytical prediction of the boundary curves for the death island regions. Using Eqs. (7) and (8), we show in Fig. 2 the analytical predictions of such boundary curves in (T, K) plane considering (a) $\rho_N = -1$ and (b) $\rho_N = -0.96$ for $T_1 = 0$ (i.e., $\delta = 0$) and $T_1 = 0.02$ (i.e., $\delta = 0.02$) with $\alpha = 1$. These values of ρ_N are those of 2-coupled oscillators ($N = 2$) [4,24] and a ring network of 11-coupled oscillators ($N = 11$), respectively [4]. In Fig. 2(a), the AD islands are in perfect agreement with those previously found using alternative theoretical (for $\delta = 0$) or numerical (for $\delta \neq 0$) approaches [4,24]. Also, the analytical results shown in Fig. 2(b) are in good agreement with the numerical predictions in a ring network of N-coupled oscillators (see Ref. [4]). The AD islands of a network of N-coupled oscillators with two time delays can be fully analytically predicted.

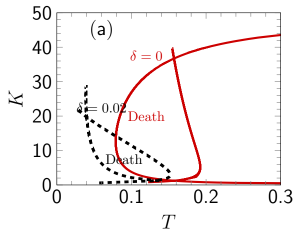

FIG. 2. Destabilizing the stable homogeneous steady state in a network of delay-coupled oscillators, Eq. (18) for (a) $N = 2$ (i.e., $\rho_1 = 1$ and $\rho_N = -1$) and (b) $N = 11$ (i.e., $\rho_1 = 1$ and $\rho_N = -0.96$) considering $\alpha = 1$. $\omega_0 = 10$ for $\delta = 0$ (i.e., $T_1 = 0$ and $T_2 = T$) and for $\delta = 0.02$ (i.e., $T_1 = 0.02$ and $T_2 = T + 0.02$).

While previous studies have focused on the cases for which $\alpha = 1$ (see Refs. [4,34–37]) or $\alpha \leqslant 1$ (see Ref. [24]), we further use Eqs. (7) and (8) to search the boundaries of AD when α is slightly greater than 1. This case corresponds to that for which the flow of information from the oscillator j is slightly smaller than that to oscillator i. Figure 3 depicts the spread of the stable HSS (AD) in the (T,K) space for $\delta = 0$ and $\delta = 0.02$ considering $\alpha = 1.05$. For $\delta = 0$ (i.e., $T_1 = 0$), it is seen that a small variation of α above 1 leads to a significant broadening of the AD region both for $N = 2$ and $N > 2$. Above a certain value of K (i.e., $K \approx 20$), AD always occurs for any value of T (i.e., $T_2 = T$) [Fig. 3(a)]. This is not surprising as, for $\alpha > 1$, all the individual oscillators are in a nonoscillatory state in the absence of any processing time delay. However, our results also provide the evidence that small values of δ are able to revive oscillations even for $\alpha > 1$ [Fig. 3(b)]. In particular, AD is no longer observed for large values of T (e.g., $T = 3$) for $\delta \neq 0$.

To substantially corroborate the above analysis for $\alpha > 1$, we have performed numerical simulations of Eq. (18) for $N = 2$. For $\alpha = 1.05$, Fig. 4 shows in color scale the values of $|Z_1|^2$ where they are constant over time after the transient for $\delta = 0$ (a) and $\delta = 0.02$ (b). We have considered that $|Z_1|^2$ is constant when the difference between the extrema in the time series is less than 10^{-5}. The AD corresponds to zero amplitude of $|Z_1|^2$ (i.e., $|Z_1|^2 = 0$). Both for $\delta = 0$ and $\delta = 0.02$, it is seen that the regions of AD are in excellent agreement with analytical predictions in Fig. 3.

For further showing the generality of our parametric approach, we now consider coupled oscillators with two delays, but with a different coupling topology:

$$\dot{Z}_j = (\mu_0 + i\omega_0 - |Z_j|^2)Z_j + \frac{K}{d_j}\sum_{s=1}^{N} g_{js} \times [Z_s(t - T_1) + Z_s(t - T_2)] - 2KZ_j(t). \quad (20)$$

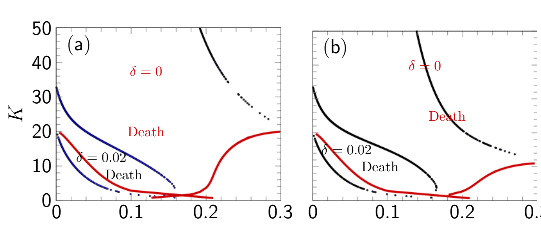

FIG. 3. Same as in Fig. 2 with $\alpha = 1.05$.

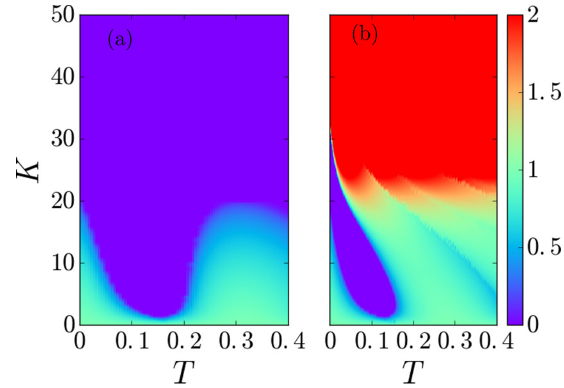

FIG. 4. Numerical simulations of Eq. (18) for $N = 2$ considering $\alpha = 1.05$ for $\delta = 0$ (a) and $\delta = 0.02$ (b). The color scale shows the values of $|Z_1|^2$.

This model is that of multiple-delay feedback control proposed by Ahlborn and Parlitz [38–40]. The model has been used to show how diffusive connections with two long-time delays can induce the stabilization of a steady state (i.e., the origin) in network oscillators [18]. The advantage of this control is that the stabilization can be achieved even if the delay times are long. For $N = 2$, the characteristic equation to ascertain the stability of the origin is given by

$$\lambda - i\omega_0 - \mu_0 + 2K - K(1 - \rho_j)[e^{-\lambda T_1} + e^{-\lambda T_2})] = 0. \quad (21)$$

The bifurcation points can be found analytically in the absence of time delay or when only one time delay is considered. In contrast, Eq. (21) has been solved numerically to determine the stability boundaries for two-delay feedback control for $N = 2$ [18]. For this specific case, we note that the values of ρ_j of interest are $\rho_1 = 0$ and $\rho_2 = 2$. Using our approach, one therefore identifies the parameters of Eqs. (7) and (8) as $Q_1 = 2K - \mu_0$, $Q_2 = \omega - \omega_0$, $R_1 = R_2 = K|1 - \rho_j|$, and $\phi_1 = \phi_2 = 0$ for ρ_1 and $\phi_1 = \phi_2 = \pi$ for ρ_2. Figure 5(a) shows the marginal stability curves estimated using formulas (7) and (8), while Fig. 5(b) shows the numerical results obtained from direct simulations of Eq. (20) in the parameter (T_1,T_2) space. Once again, an excellent agreement between analytical and numerical results is found. This further

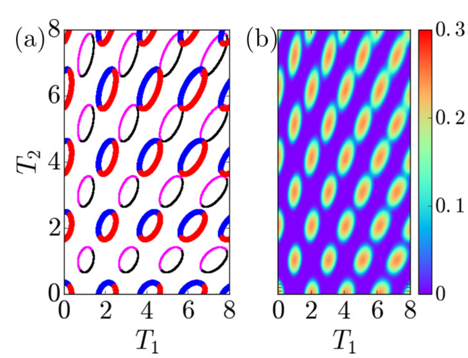

FIG. 5. (a) Marginal stability curves for the origin $z = 0$ of the pair of oscillators using formulas (7) and (8) for $\rho_1 = 0$ and $\rho_2 = 2$. The bifurcation lines surround the unstable regions. (b) Amplitudes, i.e., $|z_1|^2$, numerically obtained by integrating Eq. (18). The parameters are $N = 2$, $\mu_0 = 0.0584$, $\omega_0 = 3.0470$, and $K = 2\mu$ [18].

provides evidence to the utility of Eqs. (7) and (8) for analytical predictions of stability boundaries of coupled oscillators with two time delays. Note that, in some systems of multiple hierarchical long time delays, once the fixed points are destabilized, the spectrum can split into a pseudocontinuous part and another finite set of exponents [41]. In such a case, the number of Hopf bifurcation lines may become very large. But, the "first" Hopf line is of particular importance as it describes the moment when the whole pseudocontinuous set of eigenvalues becomes unstable. This first Hopf bifurcation line in such cases is obtained for large values of p and k in expressions (7) and (8).

IV. CONCLUSION

We have provided parametric expressions to determine critical time delays (i.e., bifurcation points) above which the stability of a given fixed point can change in nonlinear systems with one or two time delays. The concerned nonlinear systems are those for which the stability of their fixed points can be analyzed by a characteristic equation corresponding to that of scalar delay differential equations or one-component delay feedback. These parametric expressions also can be used for nonscalar differential equations with two delays provided that the characteristic equation for the stability analysis can be reduced to that of a scalar case. While such parametric expressions have been found previously for single time-delay nonlinear systems, our main contribution has been to extend such a study to the case of nonlinear systems with two time delays. The main obtained results have been applied to the paradigmatic models of dual-loop optoelectronic oscillators to draw parametrically the stability boundaries of stable microwaves. They also have been applied to identify the parameter regions of amplitude death in identical coupled oscillators with two time delays. In each case, an excellent agreement has been found either between the numerical and the analytical results or with the previously numerically reported results. Our results also have allowed for providing further evidence that processing delay in coupled oscillators is capable of reviving oscillations even when the individual oscillators are in nonoscillatory states.

ACKNOWLEDGMENTS

R.M.N. acknowledges Virginie Lecocq and Professor Thomas Erneux for fruitful discussions. He also acknowledges the fellowship from the F.N.R.S. (Belgium).

APPENDIX

For studying the stability of the nontrivial fixed point in the case of dual-loop OEOs with resonator, we introduce the small perturbations $\delta\mathcal{A}$ and $\delta\mathcal{G}_n$ satisfying $\mathcal{A}=\mathcal{A}^{\rm st}+\delta\mathcal{A}$ and $\mathcal{G}_n=\mathcal{G}_n^{\rm st}+\delta\mathcal{G}_n$, where $|\delta\mathcal{A}|\ll\mathcal{A}^{\rm st}$ and $|\delta\mathcal{G}_n|\ll\mathcal{G}_n^{\rm st}$. The first-order Taylor expansion of a perturbation of the amplitude can be determined as

$$|A^{\rm st}+\delta\mathcal{A}|\simeq A^{\rm st}+\tfrac{1}{2}[\delta\mathcal{A}+\delta\mathcal{A}^*]. \tag{A1}$$

Introducing these expressions into Eqs. (16) and (17) yields

$$\delta\dot{\mathcal{G}}_n(t)=-(\tau^{-1}+i\sigma)\delta\mathcal{G}_n+\frac{2}{\sqrt{\tau_d\tau_e}}\delta\mathcal{E}_n(t), \tag{A2}$$

$$\delta\mathcal{A}(t)=2\sum_{j=1}^{2}\beta_j\sum_{n=-\infty}^{+\infty}\left(\mathcal{G}_{n+1}^{\rm st}\delta\mathcal{G}_{n,T_j}^*+\delta\mathcal{G}_{n+1,T_j}\mathcal{G}_n^{*st}\right), \tag{A3}$$

where the prime denotes the derivative of the Bessel function with respect to its argument $A^{\rm st}$, while

$$\delta\mathcal{E}_n(t)=\tfrac{1}{2}\gamma_n(\phi)\mathrm{J}_n'(A^{\rm st})[\delta\mathcal{A}+\delta\mathcal{A}^*]. \tag{A4}$$

Note that we have set the phase factor $e^{i\nu_j}=1$ because the existence of a stationary state requires this phase factor to be real, and equal to ±1 such that γ_j is real and positive. This round-trip phase matching condition corresponds to the necessity of a constructive interference between successive round-trip replicas of the microwave (Barkhausen condition for the phase). Since $\mathcal{G}_n^{\rm st}=2\mathcal{E}_n^{\rm st}/(\sqrt{\tau_d\tau_e}(\tau^{-1}+i\sigma))$, Eq. (A3) can be rewritten as

$$\delta\mathcal{A}=2\sum_{j=1}^{2}\beta_j\sum_{n=-\infty}^{+\infty}\left(\mathcal{T}\mathcal{E}_{n+1}^{\rm st}\delta\mathcal{G}_{n,T_j}^*+\mathcal{T}^*\delta\mathcal{G}_{n+1,T_j}\mathcal{E}_n^{*st}\right), \tag{A5}$$

where $\mathcal{T}=2/(\sqrt{\tau_d\tau_e}(\tau^{-1}+i\sigma))$. Here, the index j refers to the branch j in the feedback loop. Let us first delay Eq. (A2) in time T_1 and multiply it by $2\beta_1\mathcal{T}^*\mathcal{E}_n^{*st}$. Second, we also delay the same Eq. (A2) in time T_2 and multiply it by $2\beta_2\mathcal{T}^*\mathcal{E}_n^{*st}$. Then by adding the two resulting equations and summing over all the mode indices n, one obtains

$$\begin{aligned}
\delta\dot{\mathcal{A}}_+&=-\left[\frac{1}{\tau}+i\sigma\right]\left\{\delta\mathcal{A}_+-\frac{R_1}{4}[\delta\mathcal{A}_{T_1}+\delta\mathcal{A}_{T_1}^*]-\frac{R_2}{4}[\delta\mathcal{A}_{T_2}+\delta\mathcal{A}_{T_2}^*]\right\},\\
\delta\dot{\mathcal{A}}_-&=-\left[\frac{1}{\tau}-i\sigma\right]\left\{\delta\mathcal{A}_--\frac{R_1}{4}[\delta\mathcal{A}_{T_1}+\delta\mathcal{A}_{T_1}^*]-\frac{R_2}{4}[\delta\mathcal{A}_{T_2}+\delta\mathcal{A}_{T_2}^*]\right\},\\
\delta\dot{\mathcal{A}}_+^*&=-\left[\frac{1}{\tau}-i\sigma\right]\left\{\delta\mathcal{A}_+^*-\frac{R_1}{4}[\delta\mathcal{A}_{T_1}+\delta\mathcal{A}_{T_1}^*]-\frac{R_2}{4}[\delta\mathcal{A}_{T_2}+\delta\mathcal{A}_{T_2}^*]\right\},\\
\delta\dot{\mathcal{A}}_-^*&=-\left[\frac{1}{\tau}+i\sigma\right]\left\{\delta\mathcal{A}_-^*-\frac{R_1}{4}[\delta\mathcal{A}_{T_1}+\delta\mathcal{A}_{T_1}^*]-\frac{R_2}{4}[\delta\mathcal{A}_{T_2}+\delta\mathcal{A}_{T_2}^*]\right\},
\end{aligned} \tag{A6}$$

where $\delta\mathcal{A}_{T_i}=\delta\mathcal{A}(t-T_i)$ and $\delta\mathcal{A}=\delta\mathcal{A}_+(t)+\delta\mathcal{A}_-(t)$ with

$$\delta\mathcal{A}_+(t)=2\sum_{j=1}^{2}\beta_j\sum_{n=-\infty}^{+\infty}\mathcal{G}_{n-1}^{*st}\delta\mathcal{G}_n(t-T_i), \tag{A7}$$

$$\delta\mathcal{A}_-(t)=2\sum_{j=1}^{2}\beta_j\sum_{n=-\infty}^{+\infty}\mathcal{G}_{1-n}^{\rm st}\delta\mathcal{G}_{-n}^*(t-T_i). \tag{A8}$$

Assuming $\sigma\approx0$, the variational Eq. (A6) degenerates to

$$\delta\dot{\mathcal{A}}+\text{c.c.}=-\tau^{-1}\{\delta\mathcal{A}-R_1\delta\mathcal{A}_{T_1}-R_2\delta\mathcal{A}_{T_2}\}+\text{c.c.}, \tag{A9}$$

where "c.c." denotes the complex conjugate. In order to perform the stability analysis, we assume that the perturbation $\delta\mathcal{A}$ is proportional to $e^{\lambda t}$, where $\lambda \in \mathbb{C}$. This leads to the characteristic equation:

$$\lambda + \tau^{-1}[1 - R_1 e^{-\lambda T_1} - R_2 e^{-\lambda T_2}] = 0. \tag{A10}$$

[1] D. Gosh, A. R. Chowdhury, and P. Saha, Chaos Solitons Fractals **35**, 472 (2008).
[2] X. S. Yao, L. Maleki, Y. Ji, G. Lutes, and M. Tu, in *Proceedings of the IEEE International Frequency Control Symposium (FCS '98)* (IEEE, Piscataway, NJ, 1998), pp. 545–549.
[3] R. M. Nguimdo, Y. K. Chembo, P. Colet, and L. Larger, IEEE J. Quantum Electron. **48**, 1415 (2012).
[4] W. Zou, D. V. Senthilkumar, M. Zhan, and J. Kurths, Phys. Rev. Lett. **111**, 014101 (2013).
[5] M. Mizuno and K. Ikeda, Physica D **36**, 327 (1989).
[6] C. Marriott, R. Vallée, and C. Delisle, Phys. Rev. A **40**, 3420 (1989).
[7] R. M. Nguimdo, C. Mirasso, and P. Colet, J. Quantum Electron. **46**, 1436 (2010).
[8] J. Wei and S. Ruan, Physica D **130**, 255 (1999).
[9] J. Li, Y. Kuang, and C. C. Mason, J. Theor. Biol. **242**, 722 (2006).
[10] S. Coombes and C. Laing, Philos. Trans. R. Soc. London A **367**, 1117 (2009).
[11] R. M. Nguimdo, P. Colet, L. Larger, and L. Pesquera, Phys. Rev. Lett. **107**, 034103 (2011).
[12] S. Yanchuk and G. Giacomelli, Phys. Rev. Lett. **112**, 174103 (2014).
[13] R. M. Nguimdo and P. Colet, Opt. Express **20**, 25333 (2012).
[14] M. Lakshmanan and D. V. Senthilkumar, *Dynamics of Nonlinear Time-Delay Systems* (Springer, Berlin, 2010).
[15] J. Vaughan and W. Singhose, in *The Influence of Time Delay on Crane Operator Performance*, edited by T. Vyhlıdal, J.-F. Lafay, and R. Sipahi, Delay Systems, Advances in Delays and Dynamics 1 (Springer International Publishing, Switzerland, 2014), pp. 329–342.
[16] D. Bresch-Pietri and N. Petit, in *Implicit Integral Equations for Modeling Systems with a Transport Delay*, edited by E. Witrant *et al.*, Recent Results on Time-Delay Systems, Advances in Delays and Dynamics 5 (Springer International Publishing, Switzerland, 2016), pp. 3–21.
[17] J. Martinez-Llinas and P. Colet, Opt. Express **23**, 24785 (2015).
[18] K. Konishi, H. Kokame, and N. Hara, Phys. Lett. A **374**, 733 (2010).
[19] T. Erneux, *Applied Delay Differential Equations* (Springer, New York, 2009).
[20] T. Erneux and P. Glorieux, *Laser Dynamics* (Cambridge University Press, Cambridge, UK, 2010).
[21] Y. K. Chembo, L. Larger, and P. Colet, IEEE J. Quantum Electron. **44**, 858 (2008).
[22] R. M. Nguimdo, V. Lecocq, T. Erneux, and Y. K. Chembo, J. Quantum Electron. **52**, 6500107 (2016).
[23] H. L. Smith, *An Introduction to Delay Differential Equations with Applications to the Life Sciences* (Springer, New York, 2010).
[24] W. Zou, D. V. Senthilkumar, R. Nagao, I. Z. Kiss, Y. Tang, A. Koseska, J. Duan, and J. Kurths, Nat. Commun. **6**, 7709 (2015).
[25] A. Koseska, E. Volkov, and J. Kurths, Europhys. Lett. **85**, 28002 (2009).
[26] R. Szalai and G. Orosz, Phys. Rev. E **88**, 040902 (2013)
[27] D. V. R. Reddy, A. Sen, and G. L. Johnston, Phys. Rev. Lett. **80**, 5109 (1998).
[28] K. Engelborghs, T. Luzyanina, and D. Roose, ACM Trans. Math. Softw. **28**, 1 (2002).
[29] K. Gu, S.-I. Niculescu, and J. Chen, J. Math. Anal. Appl. **311**, 231 (2005).
[30] O. D'Huys, R. Vicente, J. Danckaert, and I. Fischer, Chaos **20**, 043127 (2010).
[31] A. Coillet, R. Henriet, P. Salzenstein, K. P. Huy, L. Larger, and Y. K. Chembo, IEEE J. Sel. Top. Quantum Electron. **19**, 6000112 (2013).
[32] R. M. Nguimdo, K. Saleh, A. Coillet, G. Lin, R. Martinenghi, and Y. K. Chembo, J. Quantum Electron. **51**, 6500308 (2015).
[33] K. Saleh, R. Henriet, S. Diallo, G. Lin, R. Martinenghi, I. V. Balakireva, P. Salzenstein, A. Coillet, and Y. K. Chembo, Opt. Express **22**, 32158 (2014).
[34] D. G. Aronson, G. B. Ermentrout, and N. Kopell, Physica D **41**, 403 (1990).
[35] M. Y. Kim, R. Roy, J. L. Aron, T. W. Carr, and I. B. Schwartz, Phys. Rev. Lett. **94**, 088101 (2005).
[36] A. Prasad, Y. C. Lai, A. Gavrielides, and V. Kovanis, Phys. Lett. A **318**, 71 (2003).
[37] W. Zou, D. V. Senthilkumar, J. Duan, and J. Kurths, Phys. Rev. E **90**, 032906 (2014).
[38] A. Ahlborn and U. Parlitz, Phys. Rev. Lett. **93**, 264101 (2004).
[39] A. Ahlborn and U. Parlitz, Phys. Rev. E **72**, 016206 (2005).
[40] A. Ahlborn and U. Parlitz, Opt. Lett. **31**, 465 (2006).
[41] S. Yanchuk and G. Giacomelli, J. Phys. A **50**, 103001 (2017).